doi.org/10.26434/chemrxiv.12535913.v1

Computational Identification of Drug Lead Compounds for COVID-19 from Moringa Oleifera

Dr. Divya Shaji

Submitted date: 22/06/2020 • Posted date: 24/06/2020

Citation information: Shaji, Dr. Divya (2020): Computational Identification of Drug Lead Compounds for COVID-19 from Moringa Oleifera. ChemRxiv. Preprint. https://doi.org/10.26434/chemrxiv.12535913.v1

Molecular docking studies with the compounds from Moringa Oleifera against Mpro and RdRp. The Molecular docking was performed using AutoDock Vina. The results indicated that, the compounds pterygospermin, kaempferol,morphine and quercetin exhibited best binding energy against Mpro and RdRp.

Computational Identification of drug lead compounds for COVID-19 from *Moringa Oleifera*

Divya Shaji

Independent Researcher, India

email: divyas.bioinfo@gmail.com

Abstract

COVID-19 which is caused by the virus SARS-CoV-2, has now been declared a global pandemic by the World Health Organization. At present, no specific vaccines or drugs are available to treat COVID-19. Therefore, there is an urgent need for the identification of novel drug lead compounds to treat COVID-19. The SARS-CoV-2 main protease (M^{pro} also known as $3CL^{pro}$) and RNA-dependent RNA polymerase (RdRp also known as nsp12) are the best-characterized drug targets among corona viruses. In order to discover the natural lead compounds for SARS-CoV-2, we performed molecular docking with the compounds from *Moringa Oleifera* that target the M^{pro} and RdRp. The molecular docking studies were carried out using AutoDock Vina through PyRx. Drug-likeness property of the selected compounds was checked by applying the 'Lipinski's rule of five' using Swiss ADME. The top four compounds with most favourable binding affinity were selected for each of the targets. The results indicated that the compounds kaempferol, pterygospermin, morphine and quercetin exhibited best binding energy towards M^{pro} and RdRp. This study suggests that these natural compounds could be promising candidates for further evaluation of Covid-19 prevention.

Keywords:-COVID-19, SARS-CoV-2 main protease**,** RNA-dependent RNA polymerase, molecular docking**,** Moringa Oleifera.

1. Introduction

Severe acute respiratory syndrome corona virus (SARS-CoV-2) is a new viral infection that was first reported in China at the end of Dec 2019, raised global health concerns. WHO publicly declared the SARS-CoV-2 outbreak as a pandemic on March 11th 2020 [1]. The disease caused by SARS-CoV-2 is called COVID-19 [2], which can spread from person to person. No specific antiviral drugs have been approved for the treatment of COVID-19. Currently, several clinical trials are undergoing to identify the drugs. In this scenario, there is a need to identify novel drug lead compounds for treating COVID-19.

The SARS-CoV-2 main protease (M^{pro} also known as $3CL^{pro}$) and RNA-dependent RNA polymerase (RdRp also known as nsp12) are the best-characterized drug targets among corona viruses. These are the key components of corona virus, play an important role in mediating viral replication and transcription. Therefore, inhibition of the activity of these targets is necessary for the blockage of viral replication [2,3,4]. RdRp is considered a primary target for nucleotide analog antiviral inhibitors such as remdesivir, which shows potential for the treatment of COVID-19 viral infections [4]. This study made an attempt to find out whether the compounds from *Moringa Oleifera* (MO) inhibit these two drug targets.

Moringa Oleifera, a plant from the family *Moringacea* and its origin is in India. It is commercially grown in Africa, Mexico, America, Hawali and throughout Asia. This plant has been studied for its health properties, possesses antifungal, antioxidant, antibacterial, anti-inflammatory, diuretic and hepato protective activities. The antiviral property of *Moringa Oleifera* in *Huh7* cells was reported in a previous study [5]. The bioactive compounds that have been isolated from MO include phenolic acids, flavonoids, alkaloids, vitamins, tannins, saponins, and isothiocyanates. The roots, bark, gum, leaf, fruit (pods), flowers, seed, and seed oil of MO are reported to have various biological activities [6,7,8,9,10]. It has been reported to improve hepatic and renal functions and the regulation of thyroid hormone status [6,10].

A molecular docking study was performed with the compounds from MO using AutoDock Vina [11]. The results showed that the compounds kaempferol, pterygospermin, morphine and quercetin exhibited best binding energy towards Mpro and RdRp.

2. Methods

2.1 Collection of the ligands

Compounds isolated from the various parts of *Moringa Oleifera* were collected from the literature [6,7,8,9,10]. The initial dataset contained 33 compounds which were filtered through the "Lipinski's rule of five" [12]. SwissADME server [13] was used to calculate the "Lipinski's rule of five". Out of 33, 21 compounds were not satisfied the Lipinski's rule. The final dataset contained 12 compounds and their 3D structures in SDF format were obtained from the PubChem database [14]. The total polar surface area (TPSA) and the number of rotatable bonds were also calculated using SwissADME [13].

2.2 Molecular Docking

The 3D structures of target proteins Mpro [3] and RdRp [4] were downloaded from the PDB [15]. Molecular docking studies were performed by using AutoDock Vina [11] which is available in PyRx [16]. The target structures were converted to pdbqt format using PyRx which automatically removes the solvent molecules followed by hydrogen addition and gasteiger charges calculations [16]. The compounds in SDF format were converted to pdbqt with the help of Openbabel [17] which is available in PyRx [16]. During the docking process, the number of binding modes was set to 9 and the exhaustiveness value set to 8. For M^{pro}, the grid box size was set to 51.37, 66.97, 59.61 Å and the grid centre was set to -26.28, 12.60, 58.96 Å for x, y and z, respectively. For RdRp, the grid box size was set to 74.81, 84.54, 85.72 Å and the grid centre was set to 120.05, 123.86, 120.15 Å for x, y and z, respectively.

2.3 Analysis of the docked complexes

After docking, top hit compounds were ranked based on the least binding energy. The generated docked complexes and their binding site residues were visualised using BIOVIA Discovery studio visualizer [18]. 2D structures of the docked complexes were produced by LIGPLOT and their bonding interaction patterns (hydrogen, and hydrophobic) were examined [19].

3. Results and discussion

3.1 Molecular docking

A molecular docking study was employed to find the natural inhibitors from MO against M^{pro} and $RdRp$. The 3D structures of M^{pro} (PDB ID: 6LU7) and RdRp (PDB ID: 6M71) were retrieved from PDB [15] and docked with the 12 compounds from MO. These compounds with their binding energy values are listed in supplementary Table 1. A blind docking was performed using AutoDock Vina [11] through PyRx [16]. Docking without any assumption about the binding site is called blind docking. Nine conformations for each compound were generated and the top four compounds were selected based on the lowest binding energy (kcal/mol). The binding energies of the shortlisted compounds against Mpro and RdRp are shown in Table 1. Furthermore, the docked complexes were visualized by BIOVIA Discovery studio visualizer [18] to analyze the binding site residues. 2D structures of the docked complexes were produced by LIGPLOT to display various interactions involved in the ligand-target docking [19].

3.2 SARS-CoV-2 main protease (M^{pro} or $3CL^{pro}$)

After docking, the interactions between main protease and the compoounds from *Moringa Oleifera* were analysed and the top 4 compounds with least binding energy were selected. The selected compounds were kaempferol, pterygospermin, morphine and quercetin. These 4 compounds showed good drug-likeness properties as presented in Table 2. Chemical structures of these compounds are shown in fig.1. Docking score of all these compounds ranged between −4.2 to −7.8 kcal/mol. In particular, compounds kaempferol and pterygospermin displayed the best potent activity against M^{pro} with a same binding energy value of −7.8 kcal/mol. The binding energies of morphine and quercetin were −7.4 kcal/mol and −7.3 kcal/mol, respectively.

3.2.1 M^{pro} - kaempferol complex

The best selected pose of M^{pro}- kaempferol docked complex (binding energy −7.8 kcal/mol) predicted by AutoDock Vina is shown in Fig. 2A. The 2D diagram showing the hydrogen bonds and hydrophobic interactions involved in M^{pro}- kaempferol complex is shown in Fig. 3A. Kaempferol formed 6 hydrogen bonds with the residues Tyr54, Leu141, Gly143, Ser144, Glu166 and Asp187. Moreover, it made hydrophobic interactions with the residues His41, Met49, Leu141, Asn142, Gly143, Cys145, His164, Met165, Glu166, Asp187, Arg188 and Gln189.

Kaempferol is found in Moringa flowers [8]. It is a flavonoid compound that naturally occurs in numerous common vegetables and fruits [20,21]. The most important feature of kaempferol is its anti-inflammatory effect. It has been reported to have beneficial effects on chronic inflammatory diseases, including intervertebral disc (IVD) degeneration, post-menopausal bone loss and colitis, and acute inflammatory diseases, including acute lung injury (ALI) [21]. Another important feature of kaempferol is the prevention of cancer. Its anti-cancer role has been demonstrated in esophageal cancer, breast cancer, cervical cancer, hepatocellular carcinoma (HCC), ovarian cancer etc. [20, 21, 22]. Moreover, kaempferol has been reported to exhibit activity against herpes simplex virus, influenza viruses (H1N1 and H9N2) and hepatitis B virus under i*n vitro* conditions [23,24,25]. Zhang et al. compared the antiviral activities of flavonol kaempferol and isoflavonoid daidzein against Japanese-encephalitis-virus (JEV). They found that kaempferol exhibited more potent activity against JEV than daidzein [25]. Seo et al. investigated the antiviral effect of 10 flavonoids against two RNA viruses, namely feline calicivirus (FCV) and murine norovirus (MNV). Their findings demonstrated that kaempferol exhibited the most potent inhibitory activity against these two viruses [26, 27].

3.2.2 M^{pro} - pterygospermin complex

There were no hydrogen bonds formed between pterygospermin and M^{pro} (binding energy −7.8 kcal/mol). However, it formed hydrophobic interactions with the residues Gln110, Asn151, Ile249, Pro252, Pro293, Phe294 and Val297. 3D structure of M^{pro}-pterygospermin complex with binding site residues is shown in Fig. 2B. 2D structure of M^{pro}-pterygospermin complex with hydrogen bond and hydrophobic interactions is shown in Fig. 3B.

Pterygospermin is found in Moringa seeds. It is involved in the treatment of hyperthyroidism, chrohn's disease, arthritis, rheumatism, epilepsy, gout and cramp [8].

3.2.3 M^{pro} - morphine complex

In M^{pro}- morphine complex (binding energy −7.4 kcal/mol), the ligand is bound to the active site by forming 6 hydrogen bonds and several hydrophobic interactions. Morphine formed hydrogen bonds with His41, Leu141, Gly143, Ser144 and Cys145. The residues involved in forming hydrophobic contacts were His41, Leu141, Asn142, Gly143, Ser144, Cys145, His163, His164, Met165, Glu166 and Gln189. 3D structure of M^{pro}-morphine complex with binding site residues is shown in Fig. 2C. 2D structure of M^{pro}-morphine complex with hydrogen bond and hydrophobic contacts is shown in Fig. 3C.

Morphine is found in moringa root bark. It is an antiulcer and antiinflammatory agent [8]. Moosavi et al. investigated the inhibitory effect of morphine on growth and replication of HSV (Herpesviridae) in Vero cells. They determined the viability of cells and they found that virus particles in the infected cells was completely disappeared in the presence of morphine. However, the exact mechanism was unknown [28].

3.2.4 M^{pro}- quercetin complex

In the case of M^{pro}-quercetin complex (binding energy −7.3 kcal/mol), the results showed 7 hydrogen bonds and numerous hydrophobic contacts. The residues involved in hydrogen bond interactions were Leu141, Gly143, Ser144, Cys145 and His163. The residues participated in hydrophobic interactions were Phe140, Leu141, Asn142, Gly143, Ser144, Cys145, His163, Met165, Arg188 and Gln189. 3D structure of M^{pro}- quercetin complex with binding site residues is shown in Fig. 2D. 2D structure of M^{pro}-quercetin complex with hydrogen bond and hydrophobic contacts is shown in Fig. 3D.

Quercetin is found in Moringa flowers [8]. It is a flavonoid present in many components of human diet, it is seen in many Chinese herbs, vegetables and fruits, as well as red wine [29,30]. Rojas et al. studied the effect of quercetin on different steps of the HCV life cycle in Huh-7.5 cells and primary human hepatocytes (PHH) infected with HCVcc. They noticed that in both cell types, quercetin significantly decreased the viral genome replication; the production of infectious HCV particles and the specific infectivity of the newly produced viral particles (by 85% and 92%, Huh7.5 and PHH respectively) [29]. It has been reported that quercetin display antiviral activity against several viruses. In particular, it was shown to reduce the replication of several respiratory viruses [29]. Moreover, quercetin exerts antiproliferative, antioxidative, antibacterial, and anticancer effects [30]. Wu et al. investigated the potential inhibition mechanism of quercetin against influenza virus. They demostrated that, quercetin inhibited influenza infection with a wide spectrum of strains, including A/Puerto Rico/8/34 (H1N1), A/FM-1/47/1 (H1N1), and A/Aichi/2/68 (H3N2) with half maximal inhibitory concentration (IC50) of 7.756 ± 1.097, 6.225 ± 0.467, and 2.738 ± 1.931 μg/mL, respectively [30]. Zandi et.al [31] examined the antiviral activity of four types of bioflavonoid (quercetin,daidzein, naringin and hesperetin) against dengue virus type-2. They demonstrated that only quercetin showed significant anti-DENV-2 inhibitory activities. Daidzein, naringin and hesperetin showed minimal to no significant inhibition of DENV-2 virus replication [31].

3.3 RNA-dependent RNA polymerase (RdRp)

After docking, the interactions between RdRp and the compounds from *Moringa Oleifera* were analysed and the top 4 compounds with lowest binding energy were selected. Docking score of the

compounds ranged between −4.8 to −7.6 kcal/mol. Interestingly, the top 4 compounds selected for M^{pro} interaction showed the best binding affinity towards RdRp. They were morphine (binding energy −7.6 kcal/mol) , quercetin (binding energy −7.3kcal/mol), kaempferol (binding energy −7.2 kcal/mol) and pterygospermin (binding energy −7 kcal/mol).

3.3.1 RdRp - morphine complex

In the RdRp - morphine complex (binding energy −7.6 kcal/mol), ligand is bound to the active site by forming 6 hydrogen bonds and several hydrophobic interactions. Morphine created hydrogen bonds with Thr206, Asn209, Asp218. The residues involved in forming hydrophobic contacts were Asp36, Ile37, Tyr38, Asn39, Thr206, Asp208, Asn209, Asp218 and Asp221. 3D structure of RdRp - morphine complex with binding site residues is shown in Fig. 4A. 2D structure of RdRp - morphine complex with hydrogen bond and hydrophobic contacts is shown in Fig. 5A.

3.3.2 RdRp - quercetin complex

Quercetin docked into RdRp (binding energy −7.3 kcal/mol) by the formation of 8 hydrogen bonds and several hydrophobic interactions. This compound was found to have hydrogen bonds with Ile494, Asn496, Lys500, Arg569, Gln573, Gly683 and Tyr689. Amino acids involved in hydrophobic interactions were Asn496, Lys500, Arg569, Gln573, Leu576, Lys577, Gly683, Asp684, Ala685 and Tyr689. 3D structure of RdRp - quercetin complex with binding site residues is shown in Fig. 4B. 2D structure of RdRp-quercetin complex with hydrogen bond and hydrophobic contacts is shown in Fig. 5B.

3.3.3 RdRp- kaempferol complex

In the RdRp- kaempferol complex (binding energy −7.2 kcal/mol), the results showed 2 hydrogen bonds with the residues Thr324 and Thr334. Moreover, numerous hydrophobic interactions were noticed with the residues Leu271, Tyr273, Thr324, Ser325, Pro328, Leu329, Val330 and Arg331.
3D structure of RdRp-kaempferol complex with binding site residues is shown in Fig. 4C. 2D structure of RdRp- kaempferol complex with hydrogen bond and hydrophobic interactions is shown in Fig. 5C.

3.3.4 RdRp - pterygospermin complex

There were no hydrogen bonds fomed between RdRp-pterygospermin complex (binding energy −7 kcal/mol), however many hydrophobic interactions were observed with the residues Trp617, Asp618, Tyr619, Asp760, Asp761, Lys798, Glu811, Cys813 and Ser814. 3D structure of RdRp-

pterygospermin complex with binding site residues is shown in Fig. 4D. 2D structure of RdRp-pterygospermin complex with hydrogen bond and hydrophobic interactions is shown in Fig. 5D.

Conclusion

Molecular docking is a powerful approach for structure-based drug discovery. Using molecular docking, this study made an attempt to find out whether the compounds from *Moringa Oleifera* (MO) inhibit the COVID-19 drug targets M^{pro} and RdRp. The results suggested that, the compounds kaempferol, pterygospermin, morphine and quercetin exhibited best binding energy against M^{pro} and RdRp. Therefore, these natural compounds could be promising candidates for further evaluation of COVID-19 prevention. Moreover, the M^{pro} residues Leu141, Gly143, Ser144 and Cys145 play an important role in hydrogen bond and hydrophobic interactions.

References

1. Pachetti M, Marini B, Benedetti F, Giudici F, Mauro E, Storici P, Masciovecchio C, Angeletti S, Ciccozzi M, Gallo RC, Zella D. Emerging SARS-CoV-2 mutation hot spots include a novel RNA-dependent-RNA polymerase variant. Journal of Translational Medicine. 2020 Dec; 18:1-9.
2. Zhang L, Lin D, Sun X, Curth U, Drosten C, Sauerhering L, Becker S, Rox K, Hilgenfeld R. Crystal structure of SARS-CoV-2 main protease provides a basis for design of improved α-ketoamide inhibitors. Science. 2020 Apr 24;368(6489):409-12.
3. Jin, Z., Du, X., Xu, Y. *et al.* Structure of Mpro from COVID-19 virus and discovery of its inhibitors. Nature https://doi.org/10.1038/s41586-020-2223-y (2019)
4. Gao Y, Yan L, Huang Y, Liu F, Zhao Y, Cao L, Wang T, Sun Q, Ming Z, Zhang L, Ge J. Structure of the RNA-dependent RNA polymerase from COVID-19 virus. Science. 2020 **368**: 779-782 DOI: 10.1126/science.abb7498.
5. Feustel S, Ayón-Pérez F, Sandoval-Rodriguez A, Rodríguez-Echevarría R, Contreras-Salinas H, Armendáriz-Borunda J, Sánchez-Orozco LV. Protective effects of Moringa oleifera on HBV genotypes C and H transiently transfected Huh7 cells. J. Immunol. Res. 2017;2017.
6. Vergara-Jimenez M, Almatrafi MM, Fernandez ML. Bioactive components in Moringa Oleifera leaves protect against chronic disease. Antioxidants. 2017 Dec;6(4):91.
7. Ragasa CY, Medecilo MP, Shen CC. Chemical constituents of Moringa oleifera Lam. leaves. delta. 2015;1:1a.
8. Mehra M, Jakhar N, Joshi S, Meghwal M. Phytotherapaeutic functionality of Moringa oleifera Lam. for health. International Journal of Cell Science and Molecular Biology. 2017;3(3):1-4.
9. Ragasa CY, Ng VA, Shen CC. Chemical constituents of Moringa oleifera Lam. seeds. International Journal of Pharmacognosy and Phytochemical Research. 2016;8(3):495-8.
10. Karadi RV, Palkar MB, Gaviraj EN, Gadge NB, Mannur VS, Alagawadi KR. Antiurolithiatic property of Moringa oleifera root bark. Pharmaceutical biology. 2008 Jan 1;46(12):861-5.
11. Trott O, Olson AJ. AutoDock Vina: improving the speed and accuracy of docking with a new scoring function, efficient optimization, and multithreading. J Comput Chem. 2010; 31:455-61.
12. Lipinski CA. Drug-like properties and the causes of poor solubility and poor permeability. J Pharmacol Toxicol Methods. 2000; 44:235-249.
13. Daina A, Michielin O, Zoete V. SwissADME: a free web tool to evaluate pharmacokinetics, drug-likeness and medicinal chemistry friendliness of small molecules. Sci Rep. 2017; 7:42717.
14. Kim S, Thiessen PA, Bolton EE, Chen J, Fu G, Gindulyte A, Han L, He J, He S, Shoemaker BA,Wang J. PubChem substance and compound databases. Nucleic Acids Res. 2015;44:D1202-13.
15. Berman HM, Westbrook J, Feng Z, Gilliland G, Bhat TN, Weissig H, Shindyalov IN, Bourne PE. The protein data bank. Nucleic Acids Res. 2000; 28:235-42.
16. Dallakyan S, Olson AJ. Small-molecule library screening by docking with PyRx. Methods Mol Biol. 2015; 1263:243-250
17. O'Boyle NM, Banck M, James CA, Morley C, Vandermeersch T, Hutchison GR. Open Babel: An open chemical toolbox. J Cheminform. 2011; 3:33.
18. BIOVIA DS. Discovery Studio Visualizer, version 16.1. 0.15350. Dassault Systèmes, San Diego. 2016.

19. Wallace AC, Laskowski RA, Thornton JM. LIGPLOT: a program to generate schematic diagrams of protein-ligand interactions. Protein Eng Des Sel. 1995; 8:127-34.

20. Chen AY, Chen YC. A review of the dietary flavonoid, kaempferol on human health and cancer chemoprevention. Food chem. 2013 Jun 15;138(4):2099-107.

21. Ren J, Lu Y, Qian Y, Chen B, Wu T, Ji G. Recent progress regarding kaempferol for the treatment of various diseases. Experimental and therapeutic medicine. 2019 Oct 1;18(4):2759-76.

22. Imran M, Rauf A, Shah ZA, Saeed F, Imran A, Arshad MU, Ahmad B, Bawazeer S, Atif M, Peters DG, Mubarak MS. Chemopreventive and therapeutic effect of the dietary flavonoid kaempferol: A comprehensive review. Phytotherapy research. 2019 Feb;33(2):263-75.

23. Li J, Huang H, Feng M, Zhou W, Shi X, Zhou Pn. vitro and in vivo anti-hepatitis B virus activities of a plant extract from Geranium carolinianum L. *Antiviral Res. 2008 Aug; 79(2):114-20.*

24. *Jeong HJ, Ryu YB, Park SJ, Kim JH, Kwon HJ, Kim JH, Park KH, Rho MC, Lee WS.*Neuraminidase inhibitory activities of flavonols isolated from Rhodiola rosea roots and their in vitro anti-influenza viral activities.Bioorg Med Chem. 2009 Oct 1; 17(19):6816-23.

25. Zhang T, Wu Z, Du J, Hu Y, Liu L, Yang F, Jin Q. Anti-Japanese-encephalitis-viral effects of kaempferol and daidzin and their RNA-binding characteristics. PLoS One. 2012;7(1).

26. Zakaryan H, Arabyan E, Oo A, Zandi K. Flavonoids: promising natural compounds against viral infections. Archives of virology. 2017 Sep 1;162(9):2539-51.

27. Seo DJ, Jeon SB, Oh H, Lee B-H, Lee S-Y, Oh SH, Jung JY, Choi C. Comparison of the antiviral activity of flavonoids against murine norovirus and feline calicivirus. Food Control. 2016;60:25–30.

28. Monavari SH, Shahrabadi MS. Effects of morphine on replication of herpes simplex virus type 1 and 2. African Journal of Biotechnology. 2010;9(20).

29. Rojas Á, Del Campo JA, Clement S, Lemasson M, García-Valdecasas M, Gil-Gómez A, Ranchal I, Bartosch B, Bautista JD, Rosenberg AR, Negro F. Effect of quercetin on hepatitis C virus life cycle: from viral to host targets. Scientific reports. 2016 Aug 22;6(1):1-9.
30. Wu W, Li R, Li X, He J, Jiang S, Liu S, Yang J. Quercetin as an antiviral agent inhibits influenza A virus (IAV) entry. Viruses. 2016 Jan;8(1):6.
31. Zandi K, Teoh BT, Sam SS, Wong PF, Mustafa MR, AbuBakar S. Antiviral activity of four types of bioflavonoid against dengue virus type-2. Virology journal. 2011 Dec;8(1):1-1.

Figure Legends

Figure 1
Chemical structures of the shortlisted compounds from *Moringa Oleifera* (A) kaempferol (B) pterygospermin (C) morphine (D) quercetin

Figure 2
3D structures of Mpro-ligand complexes. 3D diagram showing the binding site residues of Mpro with the ligands (A) kaempferol (B) pterygospermin (C) morphine (D) quercetin

Figure 3
2D structures of Mpro-ligand complexes. (A) 2D diagram showing the hydrogen and hydrophobic contacts formed between Mpro and ligands (A) kaempferol (B) pterygospermin (C) morphine (D) quercetin. The green and red dotted lines indicate H-bond and hydrophobic interactions, espectively. The values adjacent to the green dotted lines indicate their distance.

Figure 4
3D structures of RdRp-ligand complexes. 3D diagram showing the binding site residues of RdRP with the ligands (A) morphine (B) quercetin (C) kaempferol (D) pterygospermin.

Figure 5
2D structures of RdRp-ligand complexes. (A) 2D diagram showing the hydrogen and hydrophobic contacts formed between RdRp and ligands (A) morphine (B) quercetin (C) kaempferol (D) pterygospermin. The green and red dotted lines indicate H-bond and hydrophobic interactions, respectively. The values adjacent to the green dotted lines indicate their distance.

Table 1: Binding energies of the selected compounds

Compound	PubChem CID	Binding energy against M^{pro} (kcal/mol)	Binding energy against RdRp (kcal/mol)
Kaempferol	5280863	−7.8	−7.2
Pterygospermin	72201063	−7.8	−7
Morphine	5288826	−7.4	−7.6
Quercetin	5280343	−7.3	−7.3

Table 2: Molecular properties of the selected compounds

Compound	H-bond acceptors	H-bond donors	MLOGP	Rotatable bonds	Molecular weight (g/mol))	TPSA ($Å^2$)
Kaempferol	6	4	−0.03	1	286.24	111.13
Pterygospermin	2	0	2.68	4	406.52	89.12
Morphine	4	2	1.74	0	285.34	52.93
Quercetin	7	5	−0.56	1	302.24	131.36

Supplementary Table 1

Binding energies of the compounds from *Moringa Oleifera* against M^{pro} and RdRP

PubChem ID	BE against Mpro	BE against RdRP
243	-5.6	-5.5
370	-5.5	-5.8
2346	-4.2	-4.8
129556	-6.2	-6.2
5280343	-7.3	-7.3
5280863	-7.8	-7.2
5288826	-7.4	-7.6
10023860	-6.6	-6.7
10088810	-6.4	-6.5
10247749	-6.5	-6.6
10426197	-6.5	-6.4
72201063	-7.8	-7

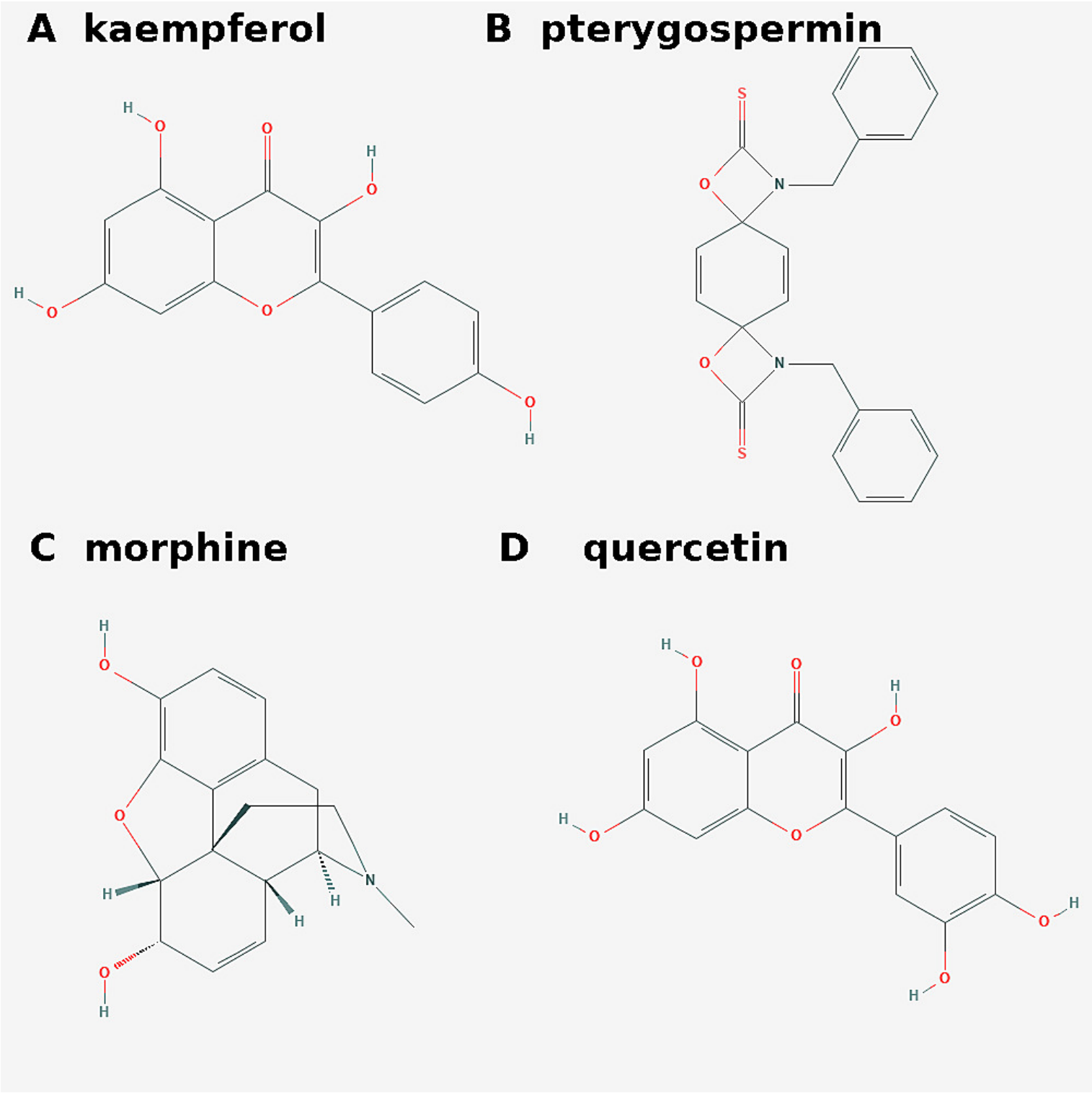

fig1.tiff (25.29 KiB) view on ChemRxiv • download file

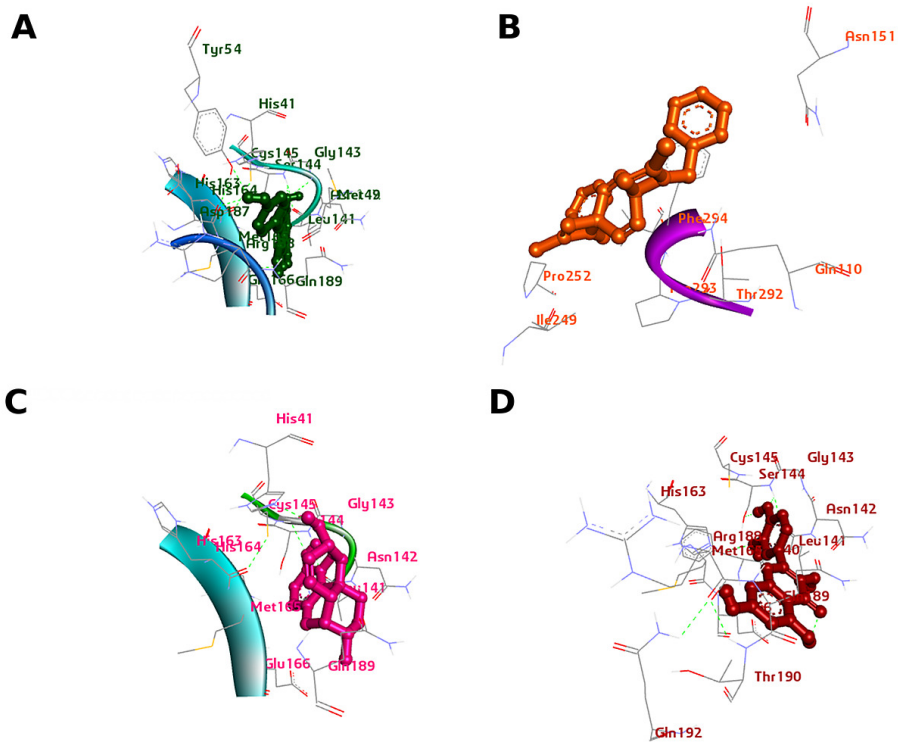

fig2.tiff (1.39 MiB)

view on ChemRxiv • download file

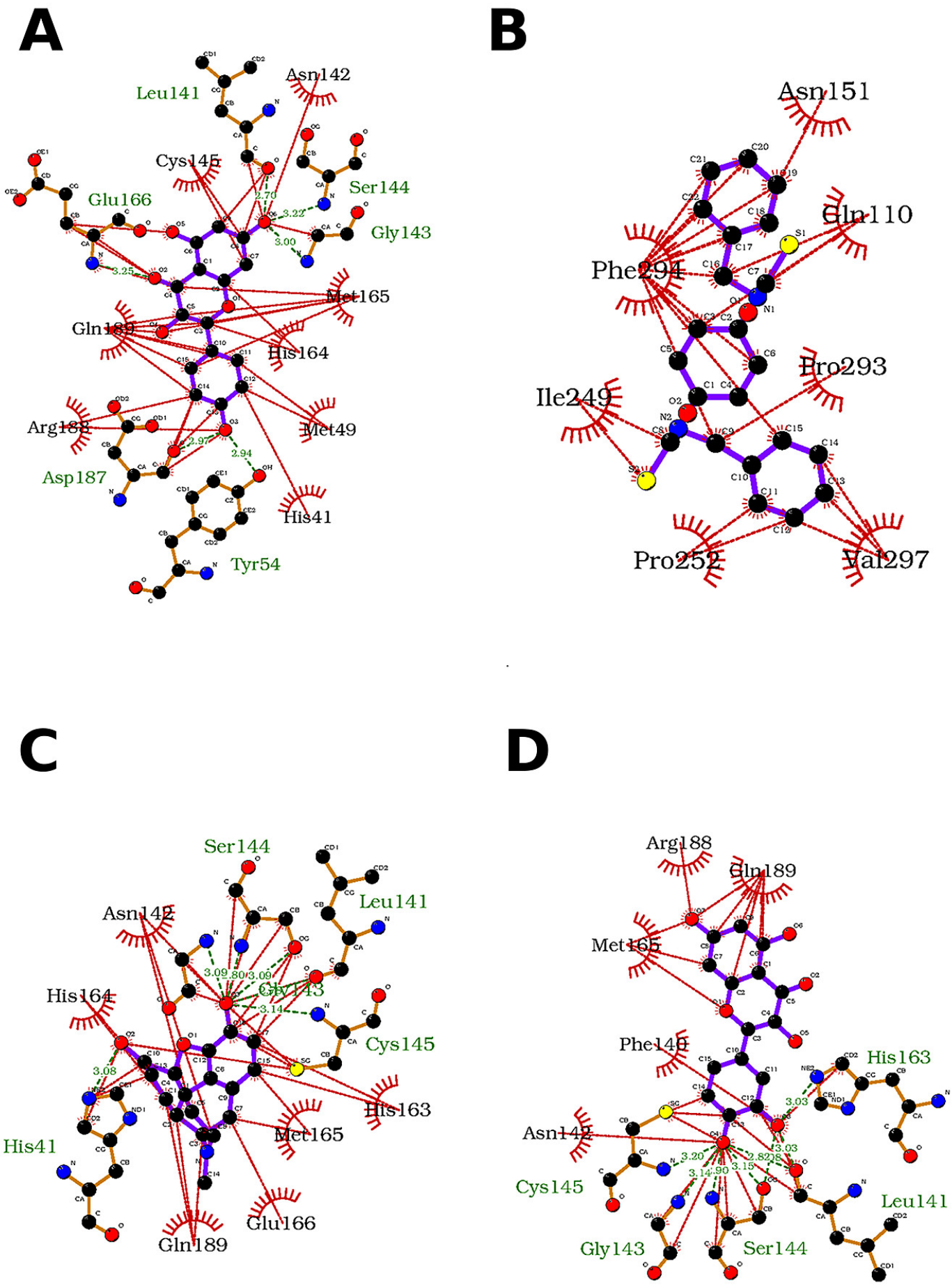

fig3.tiff (3.43 MiB)

view on ChemRxiv • download file

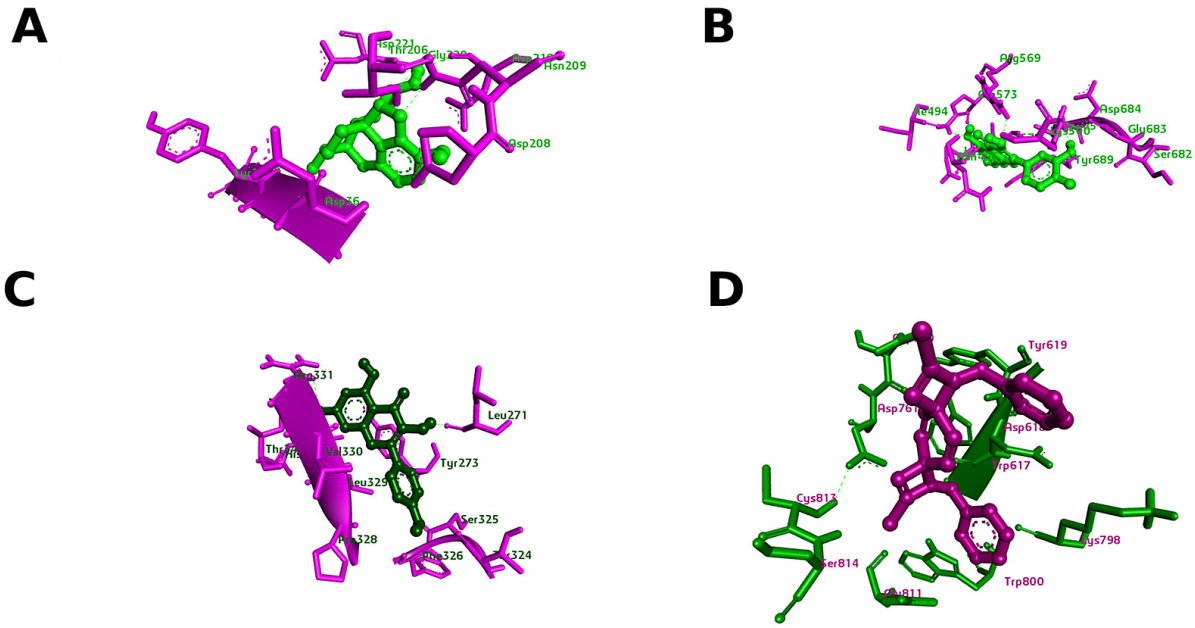

fig4.tiff (1.05 MiB)

view on ChemRxiv • download file